Available online at www.sciencedirect.com
SCIENCE DIRECT®
ELSEVIER
Journal of Magnetism and Magnetic Materials 301 (2006) 352–358
Journal of magnetism and magnetic materials
www.elsevier.com/locate/jmmm

Magnetic structure of $TbNiAl_4$

W.D. Hutchison[a,*], D.J. Goossens[b], K. Nishimura[c], K. Mori[c], Y. Isikawa[c], A.J. Studer[d]

[a]*School of Physical, Environmental and Mathematical Sciences, The University of New South Wales, Australian Defence Force Academy, Canberra, ACT 2600, Australia*
[b]*Research School of Chemistry, Australian National University, Canberra, ACT 0200, Australia*
[c]*Faculties of Engineering and Science, Toyama University, Toyama 930 8555, Japan*
[d]*Bragg Institute, Australian Nuclear Science and Technology Organisation, Lucas Heights, NSW 2234, Australia*

Received 18 May 2005; received in revised form 21 June 2005
Available online 15 August 2005

Abstract

Magnetisation and specific heat measurements, in the range 2 K to room temperature, demonstrate that three magnetic phases exist for the intermetallic compound $TbNiAl_4$. Powder neutron diffraction, also carried out over a wide temperature range, establishes that the intermediate magnetic phase is incommensurate, and confirms that the lowest temperature phase has a linear antiferromagnetic structure with a (0 1 0) propagation vector. The respective transition (Néel) temperatures, in zero applied magnetic field are 34.0 and 28.0 K.

PACS: 61.12.Ld; 75.30.Kz; 75.40.Cx

Keywords: Rare-earth ternary compounds; Neutron diffraction; Magnetism; Specific heat

1. Introduction

The rare earth series, $RNiAl_4$ (R = Y, lanthanide) forms with the orthorhombic (space group #63, Cmcm) $YNiAl_4$-type structure in which the R and Ni atoms each occupy single crystallographic sites [1,2]. Some of the initial interest in this family of compounds was via the study of the Kondo effect in $CeNiAl_4$ [3], a compound which does not show magnetic order. In contrast, $PrNiAl_4$ [4] and $NdNiAl_4$ [5] order antiferromagnetically (T_N 8.1 and 9.5 K, respectively) and also display metamagnetism. Magnetisation and susceptibility measurements on single crystals showed that the Nd compound orders along the *b*-axis whilst the Pr compound orders along the *a*-axis. Additionally, powder neutron diffraction of $PrNiAl_4$, collected

*Corresponding author. Tel.: +61 2 6268 8804; fax: +61 2 6268 8786.
E-mail address: w.hutchison@adfa.edu.au (W.D. Hutchison).

0304-8853/$ - see front matter © 2005 Elsevier B.V. All rights reserved.
doi:10.1016/j.jmmm.2005.07.012

down to 4.6 K, confirmed a linear antiferromagnetic structure with moments along the *a*-axis and a (0 1 0) propagation vector [4]. In a more recent work, the different magnetic anisotropies of the Nd and Pr in a mixed rare earth compound, $Pr_{1-x}Nd_xNiAl_4$ were examined [6]. An additional outcome of this study was the observation of a third magnetic phase at intermediate temperature, in low magnetic field, apparent for all values of x studied except $x = 1$ ($NdNiAl_4$). However, since the ordering temperatures of these $RNiAl_4$ compounds containing the light rare earths Nd and Pr are relatively low, so to the extent of the temperature range of the intermediate phase is also quite limited. For example, with $x = 0$ ($PrNiAl_4$) T_N and T_N' were found to be 8.1 and 6.9 K respectively [6]. Bulk measurements (magnetisation and specific heat) presented in this paper show that the case of the heavy rare earth Tb in $TbNiAl_4$, has broadly similar magnetic behaviour to $PrNiAl_4$. However, given the larger intrinsic magnetic moment of the Tb^{3+} ion, the magnetic phase transitions occur at higher temperature. Moreover, there is an increased temperature range for the intermediate phase, making $TbNiAl_4$ more amenable to a neutron diffraction study of the nature of this intermediate magnetic phase.

2. Experimental detail

All of the bulk measurements in this work used single crystals grown by the Czochralski pulling method using an induction furnace with an argon atmosphere. $TbNiAl_4$ starting material had been synthesised previously by repeated argon arc melting of stoichiometric amounts of 99.9% Tb together with 99.99% Ni and Al. The resulting compound was checked for impurity phases by powder X-ray diffraction (XRD). Single crystal samples were spark-cut to appropriate sizes and the crystallographic orientation was determined by Laue X-ray back reflection. Magnetisation measurements were made using a SQUID magnetometer in applied magnetic fields up to 7 T and in the temperature range from 2 to 300 K. Specific heat was measured in zero magnetic field using an adiabatic method with a mechanical heat switch employed to cool the sample and NbTi superconducting electrical leads.

The powder specimen for neutron diffraction was prepared by grinding remanent $TbNiAl_4$ single crystal pieces. Phase integrity was checked with powder XRD before powder neutron diffraction data were collected using the MRPD at the HIFAR reactor, Lucas Heights. Use of a closed cycle refrigerator allowed these measurements for temperatures ranging from 14.4 to 290 K. Data were analysed using Rietica [7] and FullProf [8], the latter allowing for refinement of magnetic structures.

3. Results

3.1. Magnetisation and specific heat

Magnetisation data collected for a $TbNiAl_4$ single crystal from 2 up to 290 K in an applied field of 1 T is shown in Fig. 1. Antiferromagnetic order along the *a*-axis is apparent at lower temperatures. The low temperature region of the *a*-axis data is expanded in the inset where the two phase

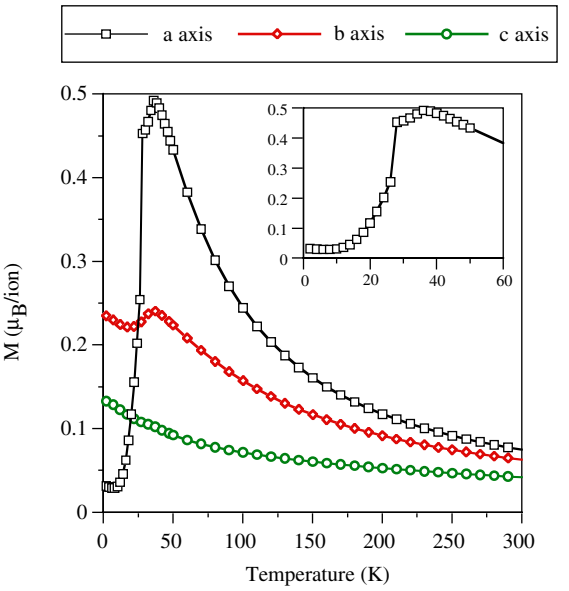

Fig. 1. Magnetisation data for a $TbNiAl_4$ crystal collected, in an applied field of 1 T, along the principal axes. The two phase transitions can be seen via the inset at 28 and 35 K.

transition temperatures T_N and T_N' (in 1 T) are close to the two abrupt changes in slope at 35 and 28 K, respectively. The temperature dependence of inverse susceptibility, also at 1 T, can be seen in Fig. 2. A linear fit to the high-temperature portion of the *a*-axis curve illustrates Curie–Weiss behaviour with the derived slope giving $C = 11.85\,\text{emu K mol}^{-1}$ ($1.489 \times 10^{-4}\,\text{m}^3\,\text{K mol}^{-1}$). This Curie constant corresponds to $\mu_{\text{eff}} = 9.73\ \mu_B$, in close agreement with $\mu_{\text{eff}} = g\sqrt{J(J+1)} = 9.72$ as expected for the Tb^{3+} ion with $J = 6$ and $g = \frac{3}{2}$ [9].

Further magnetisation measurements as a function of applied magnetic field up to 7 T, and for a range of temperatures spanning the phase transition region are in Fig. 3. Note that distinct from the three magnetic phases of this compound in the temperature manifold, three separate regions also exist, as a function of applied field, at low temperature. Fig. 3 data only illustrate the first of two transitions. The maximum net bulk moment in an applied field of 7 T is around $3\,\mu_B$, well below the Tb^{3+} free ion value of $9.0\,\mu_B$. There is a further transition to a near full moment state occurring, at low temperature, for fields beyond the range of the current measurement. At 2 K, where the first transition occurs at 5.5 T, a second transition is known to occur at around 9 T [10]. The nature of the intermediate phase in the magnetic field manifold is unclear, however the increasing hysteresis associated with the first transition with lowering temperature is suggestive of a role for domains.

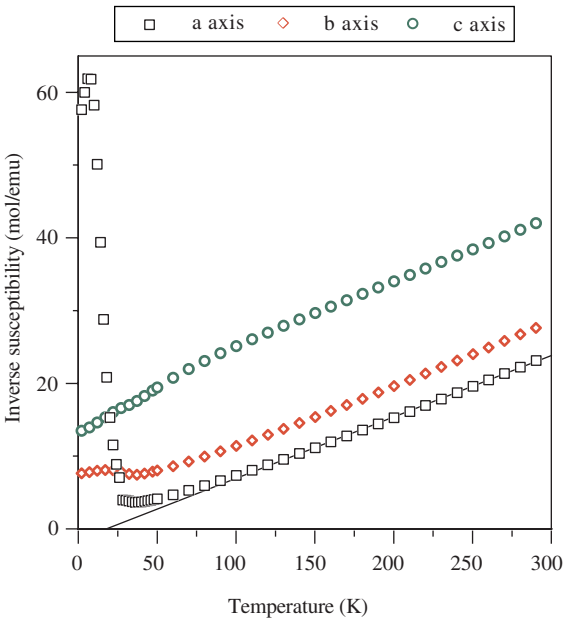

Fig. 2. Inverse susceptibility data for $TbNiAl_4$ in an applied field of 1 T. The linear fit to the high-temperature *a*-axis data shows Curie–Weiss behaviour (see text for details).

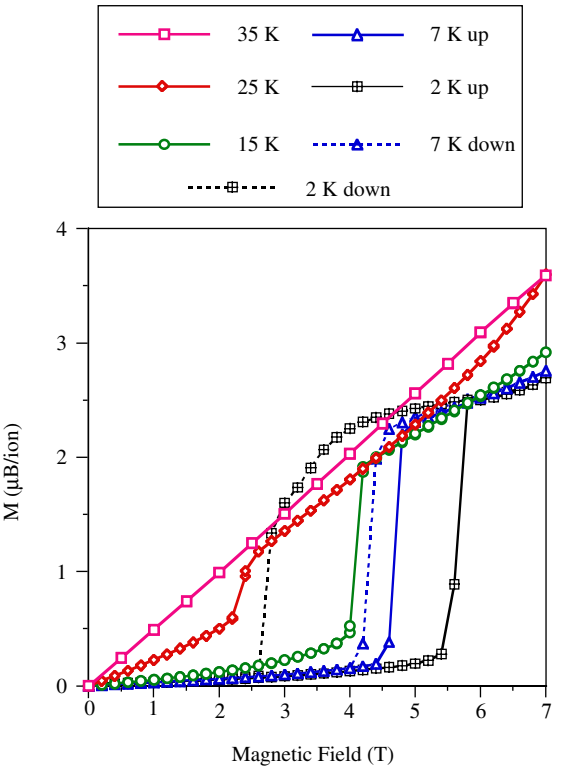

Fig. 3. Magnetisation versus applied field for $TbNiAl_4$ at various temperatures in the region of the phase transitions and below. Note that the lower temperature (2 and 7 K) data shows discernible hysteresis and the up and down sweep data are plotted separately in these cases.

The specific heat result for $TbNiAl_4$ in zero applied magnetic field is shown in Fig. 4 wherein a comparison is made with $YNiAl_4$ data that has been scaled with a mass correction of 0.8497 according to the many-Debye method [11]. These data provide a determination for $T_N = 34.0$ K and $T_N' = 28.0$ K. The difference between the $TbNiAl_4$ total curve and the lattice represented by the $YNiAl_4$ curve gives a measure of the magnetic heat capacity. The total magnetic entropy can be

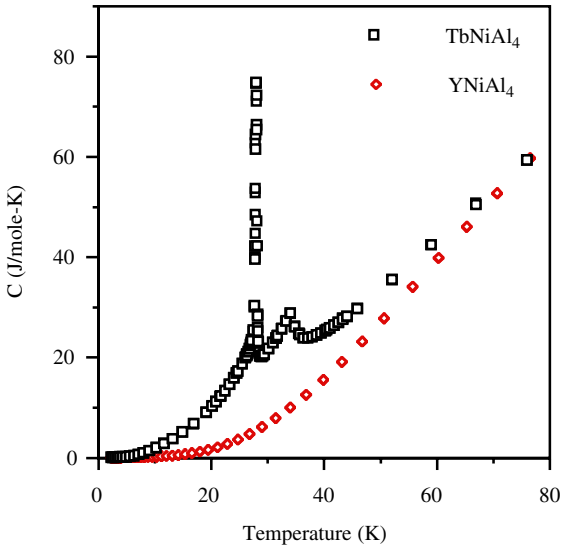

Fig. 4. Comparison of a specific heat measurement for $TbNiAl_4$ with that for $YNiAl_4$, rescaled for mass difference. Both data sets were collected in zero applied magnetic field.

evaluated by integrating over the difference in the companion C/T vs. T data. The resulting value is $16.8\,J\,K^{-1}\,mol^{-1}$ compared with $R\ln(2J+1) \approx 21.3\,J\,K^{-1}\,mol^{-1}$, with $J = 6$ for Tb^{3+}. Such a deficit in the magnetic entropy is consistent with the presence of significant CEF splitting.

3.2. Neutron diffraction

A Rietica fit to the 290 K data is shown in Fig. 5(a). High background at low angles is partly a result of the large, disordered Tb moments which are scattering isotropically. This contribution can be seen to be smaller in Figs. 5(b) and (c) where more of the moment is ordered. The magnetic form factor falls off with angle, explaining the higher background at lower angles. There is no evidence for ordered magnetic moments in this data. The structure is summarised in Table 1.

Fig. 5(c) is a FullProf fit to the diffraction data at 14.4 K. The most obvious feature is a huge peak at the (0 1 0) position of the Cmcm cell, which as can be seen from the top row of peak markers (structural phase) is not an allowed structural reflection. This implies that the magnetic structure is antiferromagnetic with a propagation vector

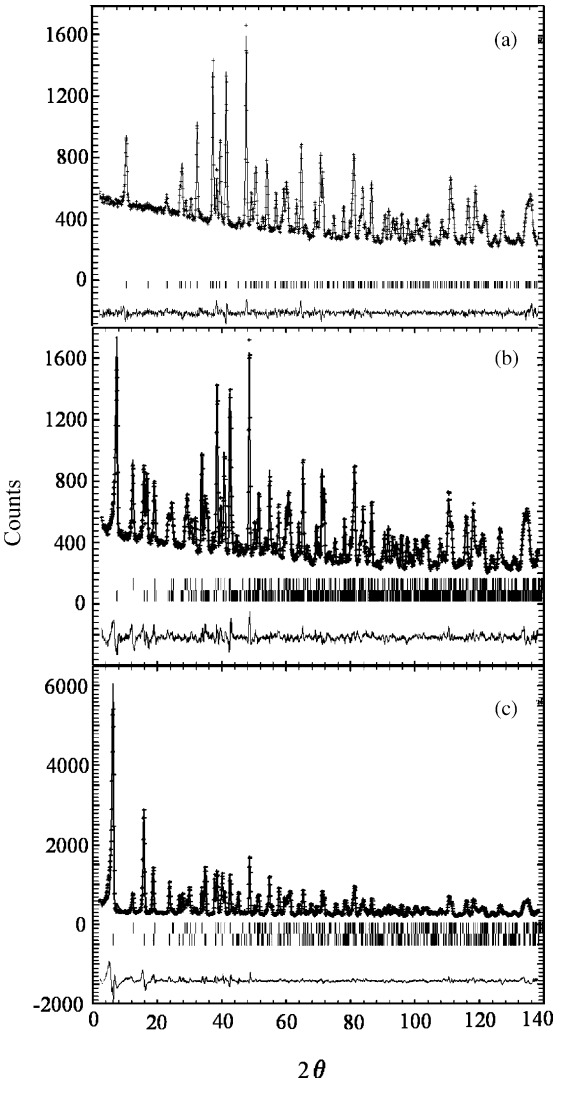

Fig. 5. (a) Rietica fit to 290 K neutron data. Note large background and lowest angle peak is at about 12°. (b) FullProf fit to 32.0 K data. New peaks compared to (a) are due to incommensurate magnetic ordering. (c) FullProf fit to 14.4 K data. Note this is on a different scale to (a) and (b). Large peak at very low angle is not well handled by asymmetry functions. In all plots vertical lines denote Bragg positions. In (b) and (c) the lower row of markers give the magnetic structure peak positions.

$\tau = (0\,1\,0)$. (The lower row of markers shows the peak positions for the magnetic structure.) Following Mizushima et al. [4] and the magnetometry results presented above, the magnetic structure model is one in which the moments are

Table 1
Structural parameters for $TbNiAl_4$ at 290 K

Atom	x	y	z	B_{iso}
Tb	0	0.1166(3)	0.25	0.40(5)
Ni	0	0.7735(5)	0.25	0.84(5)
Al1	0	0.5	0	0.85(5)
Al2	0	0.9234(6)	0.25	0.80(5)
Al3	0	0.3118(3)	0.0530(3)	0.35(5)
Space group	Cmcm			
a,b,c (Å)	4.063(3)	15.415(6)	6.603(4)	

(anti)parallel with the a lattice vector and antiferromagnetically arranged. The magnetic peaks are large, as might be expected with Tb moments ordering. Further, the (0 1 0) peak is at very low angles and the asymmetry is strong and not well corrected. This impacts on the goodness of fit, but does not affect the conclusions drawn from the analysis. The fit yields a moment of 8.3(2) μ_B, slightly below the free ion Tb^{3+} value 9.0 μ_B [9]. Such a deficit in moment magnitude is consistent with the presence of a non-negligible CEF as noted above. It can be concluded that the low-temperature magnetic structure of $TbNiAl_4$ is the same as that published for $PrNiAl_4$. Similar analyses were done on the data sets with temperatures ranging from 14.4 to 28.0 K. The staggered moment was extracted and plotted as a function of T in Fig. 6.

However, at 32.0 K a quite different magnetic structure was apparent, leading to the conclusion that the material has three phases—a low-temperature magnetic phase, an intermediate magnetic phase and the paramagnetic phase encountered at high temperature. Such a conclusion is in agreement with the magnetisation results. While the diffraction pattern collected at 32.0 K is the lowest temperature pattern to show strong incommensurate peaks, a small feature is present at 28.0 K at the position of the first incommensurate. However at 32.0 K there is absolutely no evidence of the large commensurate (0 1 0) magnetic peak. Further, a weak broad feature is apparent at the incommensurate position at 41.1 K, suggesting that the transition from paramagnetic to incommensurate periodic magnetic is second order while the onset of the commensurate phase is a first order transition. This is in accordance with the

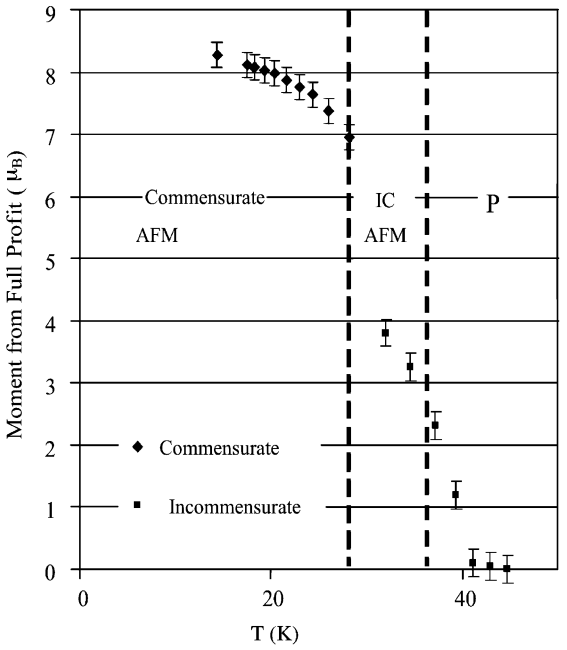

Fig. 6. Staggered moment in low-temperature region as a function of T. AFM = antiferromagnetic, P = paramagnetic, IC = incommensurate.

specific heat data (Fig. 4), which shows a very sharp strong peak at the lower transition and a much broader peak at the incommensurate to paramagnetic transition. This second peak does not occur when the incommensurate moment goes to zero but rather when the moment is falling most rapidly as a function of T. Indeed, the peak can be seen to extend almost to 40 K, which is where the incommensurate moment comes within error of zero in Fig. 6.

FullProf is capable of fitting incommensurable magnetic structures as it allows a propagation vector to be defined. An exhaustive search was done to find a propagation vector which would give the incommensurate magnetic structure. However, if it was assumed that as for the commensurate ordering, $k_\tau = 1$ for the incommensurate magnetic propagation vector τ, then the h_τ and l_τ components were linked by the propagation vector magnitude.

If

$$|\tau| = ((h_\tau a^*)^2 + b^{*2} + (l_\tau c^*)^2)^{1/2} \quad (1)$$

and $|\tau|$ can be found from the diffraction pattern, there is only one degree of freedom in the search, with a limited domain. After refining, this yielded a propagation vector $\tau = (h_\tau k_\tau l_\tau) = (0.171(2)\ 1\ 0.038(1))$ at 32.0 K, and the fit resulting from this can be seen in Fig. 5(b). Again, the largest peak is at very low angle and peak asymmetry is not well modelled, but the vector does pick up all magnetic peaks without putting intensity elsewhere.

The magnetic moment from the incommensurate fitting was found to be 3.8(2) μ_B at 32.0 K, much smaller than that from the adjacent temperature of the commensurate phase ($\sim 7\,\mu_B$ at 28.0 K). This appears to contradict the bulk measurements which show continuity in magnetisation magnitude during the transition between the magnetic phases, but allowance should be made for the significantly larger background apparent at 32.0 K due to the disordered Tb moments. Also it is evident that the magnetic intensity is much larger in the low-temperature phase. Hence it appears that the ordered moment in the incommensurate phase is not the full moment of the Tb, but that some component of the Tb moment is disordered. It is possible that the moment does change continuously between 28 and 32 K, and Mössbauer data for $GdNiAl_4$ suggest a continuous variation in that case [12]. Evidence for the incommensurate magnetic phase is not apparent at temperatures above approximately 45 K, although the magnetic peak intensities fall off very slowly with T and a cut off is difficult to determine. The largest peak is very weak at temperatures above 37.1 K, and its increased width suggests that it may not be long range ordered. The fall off of the incommensurate ordered moment with T is shown in Fig. 6, with the three magnetic phases noted.

The evolution of $|\tau|$ with T is plotted in Fig. 7. The magnitude is constant, while the h_τ and l_τ components move in opposite directions. There is no evidence of τ moving towards a commensurate value as the transition to the commensurate magnetic phase is approached, as expected for the assigned first-order nature of this phase transition. Finally, it is noted that inspection of the fits for variation of lattice parameters

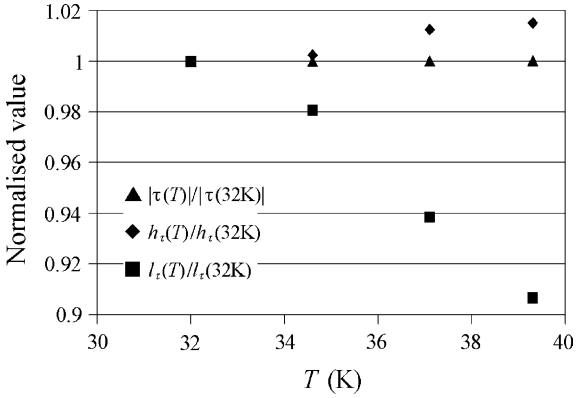

Fig. 7. Magnitude of τ, h_τ and l_τ as functions of T, each normalised to their values at 32.0 K. Symbol size indicates uncertainty.

reveals a tiny step increase in unit cell volume ($\sim$0.03%) near the lower transition temperature (between 28.0 and 32.0 K). However, this cannot be considered significant in terms of the accuracy of the data and a higher resolution experiment would be required to confirm this effect.

4. Conclusion

Magnetisation and specific heat measurements indicate that three magnetic phases exist for the intermetallic compound $TbNiAl_4$. The respective transition (Néel) temperatures, in zero applied magnetic field are 34.0 and 28.0 K. Powder neutron diffraction, also carried out over a wide temperature range confirms that the structure of the lowest temperature phase is like that of $PrNiAl_4$, namely, a linear antiferromagnetic structure with a (0 1 0) propagation vector. Also it establishes that the intermediate magnetic phase is incommensurate with propagation vector τ =(0.171(2) 1 0.038 (1)). Studies of $TbNiAl_4$ and other $RNiAl_4$ compounds using low-temperature nuclear orientation and Mössbauer spectroscopy are under way to confirm the low-temperature magnitude and variation with temperature of the rare earth moments in these compounds.

Acknowledgements

The Australian Institute of Nuclear Science and Engineering (AINSE) is gratefully acknowledged for a grant enabling the ND study. The authors thank D.H. Chaplin and G.A. Stewart for discussions and comments.

References

[1] P. Villars, Pearson's Handbook Desk Edition, ASM International, 1997.
[2] R.M. Rykhal, O.S. Zarchnyuk, Ya.P. Yarmolyuk, Sov. Phys.-Crystallogr. 17 (1972) 453 (translated from Kristallografiya).
[3] T. Mizushima, Y. Isikawa, A. Maeda, K. Oyabe, K. Mori, K. Sato, K. Kamigaki, J. Phys. Soc. Jpn 60 (1991) 753.
[4] T. Mizushima, Y. Isikawa, J. Sakurai, M. Ohashi, Y. Yamaguchi, J. Phys. Soc. Jpn 66 (1997) 3970.
[5] T. Mizushima, Y. Isikawa, T. Yasuda, T. Kuwai, J. Sakurai, J. Phys. Soc. Jpn 68 (1999) 637.
[6] K. Nishimura, T. Yasukawa, K. Mori, Y. Isikawa, W.D. Hutchison, D.H. Chaplin, Jpn. J. Appl. Phys. 42 (2003) 5565.
[7] B.A. Hunter, C.J. Howard, Rietica (available from www.ccp14.ac.uk).
[8] J. Rodriguez-Carvajal, Physica B 192 (1993) 55.
[9] G.A. Stewart, Mater. Forum 18 (1994) 177.
[10] T. Mizushima, Y. Isikawa, private communication.
[11] M. Bouvier, P. Lethuillier, D. Schmitt, Phys. Rev. B 43 (1991) 13137.
[12] G.A. Stewart, W.D. Hutchison, A.V.J. Edge, K. Rupprecht, G. Wortmann, K. Nishimura, Y. Isikawa, J. Magn. Magn. Mater. 292 (2005) 72.